Convection-permitting climate models offer more certain extreme rainfall projections

Giorgia Fosser, Marco Gaetani, Elizabeth Kendon, Marianna Adinolfi, Nikolina Ban, Danijel Belušić, Cécile Caillaud, João Careto, Erika Coppola, Marie-Estelle Demory, et al.

npj | climate and atmospheric science

Article

Published in partnership with CECCR at King Abdulaziz University

https://doi.org/10.1038/s41612-024-00600-w

Convection-permitting climate models offer more certain extreme rainfall projections

Giorgia Fosser[1] ✉, Marco Gaetani[1], Elizabeth J. Kendon[2,3], Marianna Adinolfi[4], Nikolina Ban[5], Danijel Belušić[6,7], Cécile Caillaud[8], João A. M. Careto[9], Erika Coppola[10], Marie-Estelle Demory[11,12,13,14], Hylke de Vries[15], Andreas Dobler[16], Hendrik Feldmann[17], Klaus Goergen[18], Geert Lenderink[15], Emanuela Pichelli[10], Christoph Schär[11], Pedro M. M. Soares[9], Samuel Somot[8] & Merja H. Tölle[19]

Extreme precipitation events lead to dramatic impacts on society and the situation will worsen under climate change. Decision-makers need reliable estimates of future changes as a basis for effective adaptation strategies, but projections at local scale from regional climate models (RCMs) are highly uncertain. Here we exploit the km-scale convection-permitting multi-model (CPM) ensemble, generated within the FPS Convection project, to provide new understanding of the changes in local precipitation extremes and related uncertainties over the greater Alpine region. The CPM ensemble shows a stronger increase in the fractional contribution from extreme events than the driving RCM ensemble during the summer, when convection dominates. We find that the CPM ensemble substantially reduces the model uncertainties and their contribution to the total uncertainties by more than 50%. We conclude that the more realistic representation of local dynamical processes in the CPMs provides more reliable local estimates of change, which are essential for policymakers to plan adaptation measures.

Regional climate models (RCMs) have been shown to be an important tool in climate research and are often used to drive impact models[1,2]. However, RCMs still underestimate precipitation extremes that are one important component of the water cycle[3], with implications for the reliability of future projections especially for sub-daily precipitation[4,5]. These shortcomings have been linked to the parameterisation of convection[6] – a key process behind many of our extreme weather events, including short-duration high-intensity precipitation extremes responsible for flash flooding events in summer over Europe[7]. The possibility to remove this source of uncertainty with km-scale models, called convection-permitting models (CPMs), for which deep convection is explicitly represented, could open the path to more trustworthy estimates of future changes in extreme sub-daily precipitation. Previous literature already showed that CPMs more realistically represent sub-daily statistics[6,8] and extremes leading to higher confidence on their climate projections compared to RCMs[4,9].

For an effective adaptation strategy, policy-makers need not only information on future local changes, but also an evaluation of the uncertainty associated with the climate projection. There are three main sources of

[1]University School for Advanced Studies IUSS, Pavia, Italy. [2]Met Office Hadley Centre, Exeter, UK. [3]Bristol University, Bristol, UK. [4]CMCC Foundation - Euro-Mediterranean Center on Climate Change, Caserta, Italy. [5]Department of Atmospheric and Cryospheric Sciences, University of Innsbruck, Innsbruck, Austria. [6]University of Zagreb, Zagreb, Croatia. [7]Swedish Meteorological and Hydrological Institute, Norrköping, Sweden. [8]Université de Toulouse, Météo-France, CNRS, Toulouse, France. [9]Universidade de Lisboa, Faculdade de Ciências, Instituto Dom Luiz, Lisboa, Portugal. [10]The Abdus Salam International Centre for Theoretical Physics (ICTP), Trieste, Italy. [11]Institute for Atmospheric and Climate Science, ETH Zürich, Zurich, Switzerland. [12]Wyss Academy for Nature, University of Bern, Bern, Switzerland. [13]Climate and Environmental Physics, Physics Institute, University of Bern, Bern, Switzerland. [14]Oeschger Centre for Climate Change Research, University of Bern, Bern, Switzerland. [15]Royal Netherlands Meteorological Institute KNMI, De Bilt, Netherlands. [16]Norwegian Meteorological Institute, Oslo, Norway. [17]Institute for Meteorology and Climate Research (IMK-TRO), Karlsruhe Institute of Technology (KIT), Karlsruhe, Germany. [18]Institute of Bio- and Geosciences (IBG-3, Agrosphere), Research Centre Juelich, Juelich, Germany. [19]Universität Kassel, Kassel Institute for Sustainability, Kassel, Germany. ✉e-mail: giorgia.fosser@iusspavia.it

uncertainty: the climate scenario, model uncertainty and internal variability, often called natural variability[10,11]. The first is related to the chosen socio-economic emission scenario and the underlying assumptions in terms of anthropogenic emissions, stratospheric ozone concentrations, land use change, etc. Given the same external forcing, model uncertainty arises from the use of different parameterization schemes (or parameter choices within the same model) or numerical formulations across different models. The last source of uncertainty is the natural variability of the climate system linked to its chaotic nature. The relative contribution of the various sources of uncertainty depends on several factors (e.g. analysed variables and statistics used, temporal and spatial scale considered, time frame), but the fractional uncertainty from climate scenarios becomes smaller compared to model uncertainty and internal variability moving from global to regional scale[10]. Over Europe, the choice of the RCM has a major influence on the total uncertainties for summer precipitation[12] suggesting that a correct representation of convection could lead to a reduction in uncertainties in its future response.

Little is known in terms of uncertainties of the climate change signal in CPMs given the high computational costs that constrain the possibility to run ensembles. Using a single-model CPM ensemble perturbed at the boundary, the UKCP project[13] found that the climate change signal in the CPM ensemble tends to converge, thanks to the explicit representation of convection[4]. However, a multi-model ensemble that samples different CPM model physics is necessary to confirm if a more realistic representation of the local convective dynamics (common to all CPMs) can really lead to a reduction of uncertainties for extreme summer precipitation projections.

The CORDEX Flagship Pilot Study project[14] on Convective Phenomena over Europe and the Mediterranean (FPS Convection) is a coordinated multi-model experiment setup to investigate the added-value of CPMs, as well as their climate change signal and related uncertainties in a systematic way over the greater Alpine region[14–20]. In accordance with previous literature, this CPM ensemble showed the most significant benefit compared to the driving RCMs in the representation of summer heavy precipitation and precipitation frequency at daily and hourly scales[16]. Both CPM and RCM ensembles produce similar projections, but with a tendency for larger increases in precipitation intensity in the CPMs. In particular, the ensembles project a decrease in summer mean precipitation, mainly due to a reduction of events in the future, and a decrease in the intensity of extreme events in southern Europe[15]. The spread in the CPM ensemble tends to be reduced for most of the analysed indices and areas especially in SON.

Here, we consider 9 CPM simulations (2.5–3 km) and the corresponding driving RCM, with a resolution ranging between 12 and 25 km, performed within the FPS Convection (see Methods and Table 1 for more details). Each simulation covers a 10-year time slice for present day (1996–2005) and for the end of the century (2090–2099) under the Representative Concentration Pathway (RCP) 8.5 scenario[21]. For the entire greater Alpine region, we investigate the future changes in extreme hourly precipitation statistics, focusing on summer when convection is predominant over Europe, and evaluate the uncertainty linked to the climate change signal in the CPM and RCM ensemble. Given the ensemble design, this analysis cannot consider emission scenario uncertainty. Using the bootstrap approach[22] sketched in Fig. 1, we disentangle the model uncertainty and natural variability from the total uncertainty within the RCP8.5 scenario. Then, we analyse the contributions of the model uncertainty and of the natural variability to the total uncertainty comparing the spreads in the bootstrapped ensemble (see Methods more details). The possibility to reduce the contribution of model uncertainty to the total uncertainty in CPMs would lead to higher confidence in the projection and to more reliable information for policy-makers. To verify that the results are not linked to the specific models included in the ensemble, the different statistics are repeated for a subset of models containing only one model from each family for both CPMs and RCMs.

Results

Future changes in precipitation extremes and related uncertainties

Figure 2 shows the distribution of hourly precipitation intensities over land using the fractional contribution of each intensity bin to the total summer precipitation[23,24]. Although the CPM and RCM ensembles show significantly different hourly distributions, the climate change signal is similar with both projecting a significant decrease in the contribution from low to medium precipitation intensities (below 2 mm/h and 5 mm/h for RCMs and CPMs respectively) and increase from high intensities (above 5 and 8 mm/h for RCMs and CPMs respectively) in line with previous studies[4,5,15]. This increase appears to be linked, especially for CPMs, to an intensification of short-lived high-intensity events (i.e. duration below 6 h and intensities above 10 mm/h, Fig. 3), often of convective nature[4,25], rather than to an increased frequency of intense events above 10 mm/h, which is limited (+ 0.01% for CPMs, +0.004% for RCMs, Supplementary Fig. 1).

Table 1 | List of models and institutes that contributed to the study

Institute	CPM (resolution)	RCM (resolution)	GCM
CMCC Euro-Mediterranean Center on Climate Change	CCLM5[32,33] (3 km)	CCLM5[32,33] (12 km)	EC-Earth
KIT Karlsruhe Institute of Technology	CCLM5[32,34,35] (3 km)	CCLM4[34,36] (12 km)	MPI-ESM-LR
ETH Institute for Atmospheric and Climate Science	COSMO-crCLIM[32,37] (2.2 km)	COSMO-crCLIM[32,38] (12 km)	MPI-ESM-LR
CNRM Centre National de Recherches Météorologiques	CNRM-AROME41t1[39] (2.5 km)	CNRM-ALADIN63[40] (12 km)	CNRM-CM5
DMI-MET-SMHI DMI-MET Norway- SMHI HARMONIE-Climate community	HCLIM38-AROME[41] (3 km)	HCLIM38-ALADIN[41] (12 km)	EC-Earth
KNMI The Royal Netherlands Meteorological Institute	HCLIM38-AROME[41] (2.5 km)	RACMO2.3[42] (12 km)	EC-Earth
FZJ-IBG3 & IDL Research Centre Julich & Institute Dom Luiz	WRF3.8.1CA[43] (3 km)	WRF3.8.1CA[43] (12 km)	EC-Earth
ICTP Abdus Salam Internatinal Centre for Theoretical and Earth System Physics	RegCM4[44] (3 km)	RegCM4[44] (12 km)	HadGEM
MOHC Met Office Hadley Centre Exeter	HadREM_UM10.1[24,45] (2.2 km)	—	HadGEM (25 km, atmosphere-only)

The thicker borders identify the models from the same family.

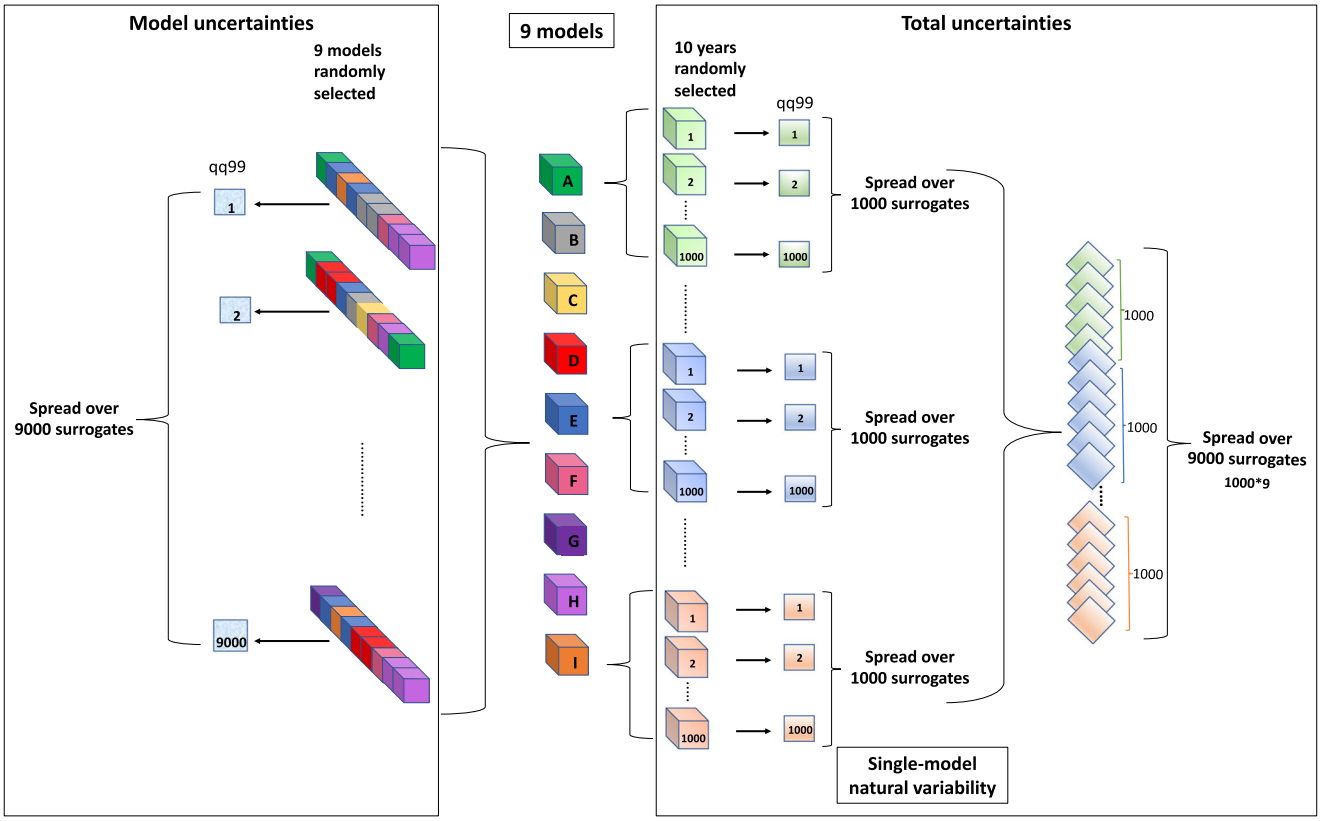

Fig. 1 | Schematic of the bootstrapping approach. The nine model simulations are shown in the centre as cuboids with the three dimensions representing longitude, latitude and time, while each vivid colour characterises a different model. The strategy is represented for the model uncertainty on the left, while on the right for the single-model natural variability and the total uncertainty. The squares represent the results of the statistic, e.g. heavy precipitation (p99), calculated over the time thus reducing the cuboid (bootstrap surrogate) to two dimensions, i.e. longitude and latitude. The spread, calculated as the interval between the 2.5th and 97.5th quantiles of the surrogates, is the measure of each uncertainty.

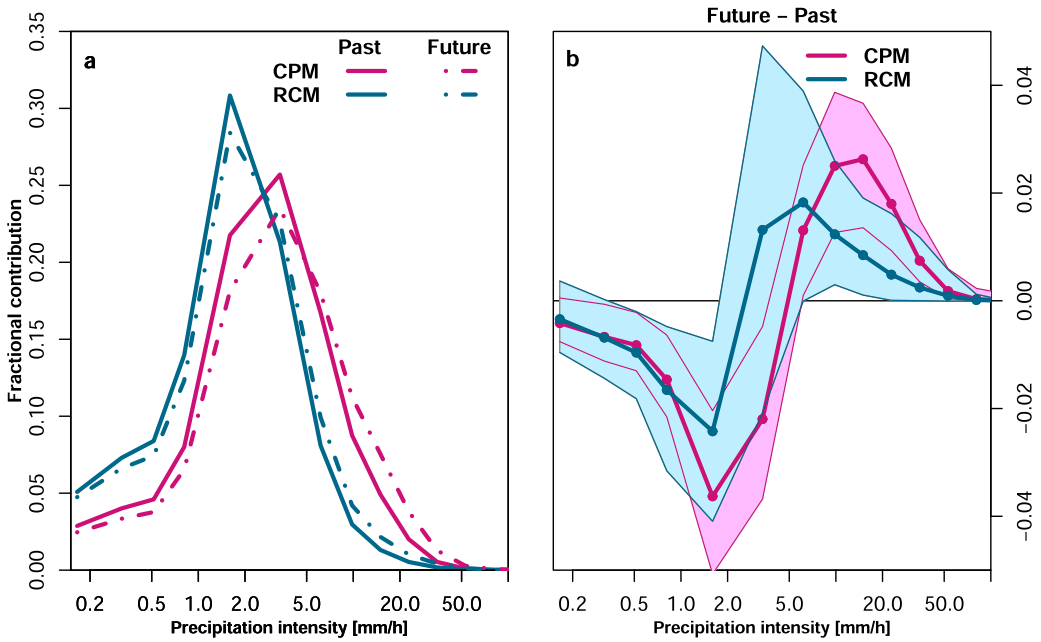

Fig. 2 | Fractional contribution of hourly precipitation intensities to the total precipitation. The figure refers only to land grid points in summer for the CPM (purple) and RCM (petroleum) ensemble mean for the past and future times slices (**a**, solid and dashed lines respectively) and future changes (**b**), where the coloured areas represent the 97.5th confidence interval and the significant changes at the 95th level are indicate by solid dots. Note the logarithmic x axis. The bins are 0, 0.10, 0.23, 0.41, 0.62, 0.10, 2.20, 4.52, 7.79, 11.87, 18.08, 27.54, 41.96, 63.94, 97.41, 148.41, 350.00.

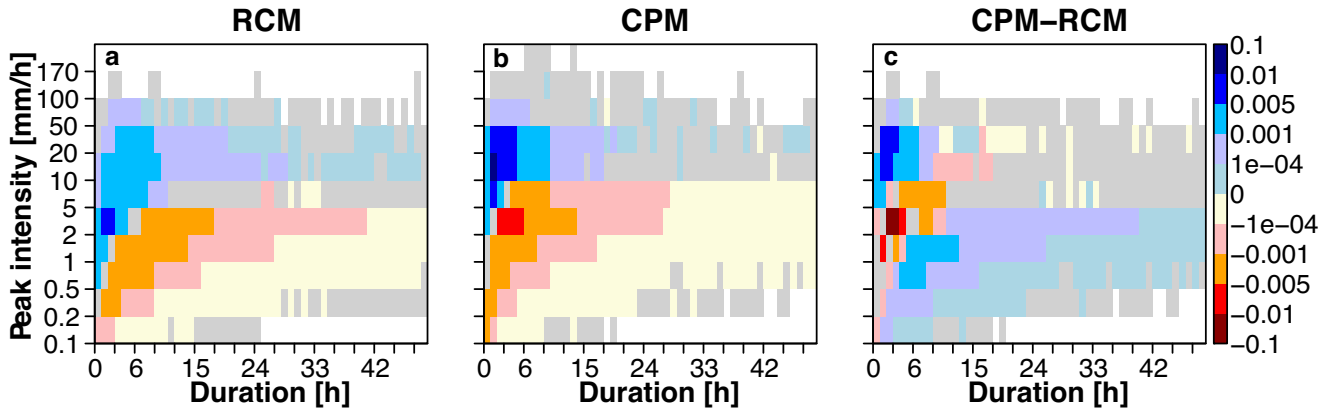

Fig. 3 | Summer changes in the precipitation events characteristics. Future change in the contribution to the total precipitation is defined as a function of the peak precipitation intensity and duration of precipitation event, where an event is defined as a continuous period of precipitation exceeding 0.1 mm/h, for the ensemble mean of RCM (**a**), CPM (**b**) and CPM-RCM difference (**c**). Fractional contribution is given by (joint probability of a given amount-duration bin) × (mean bin precipitation amount) / (total precipitation over all bins), pooling all land points over the domain. Future changes or differences that are not significant at the 5% level are masked in grey.

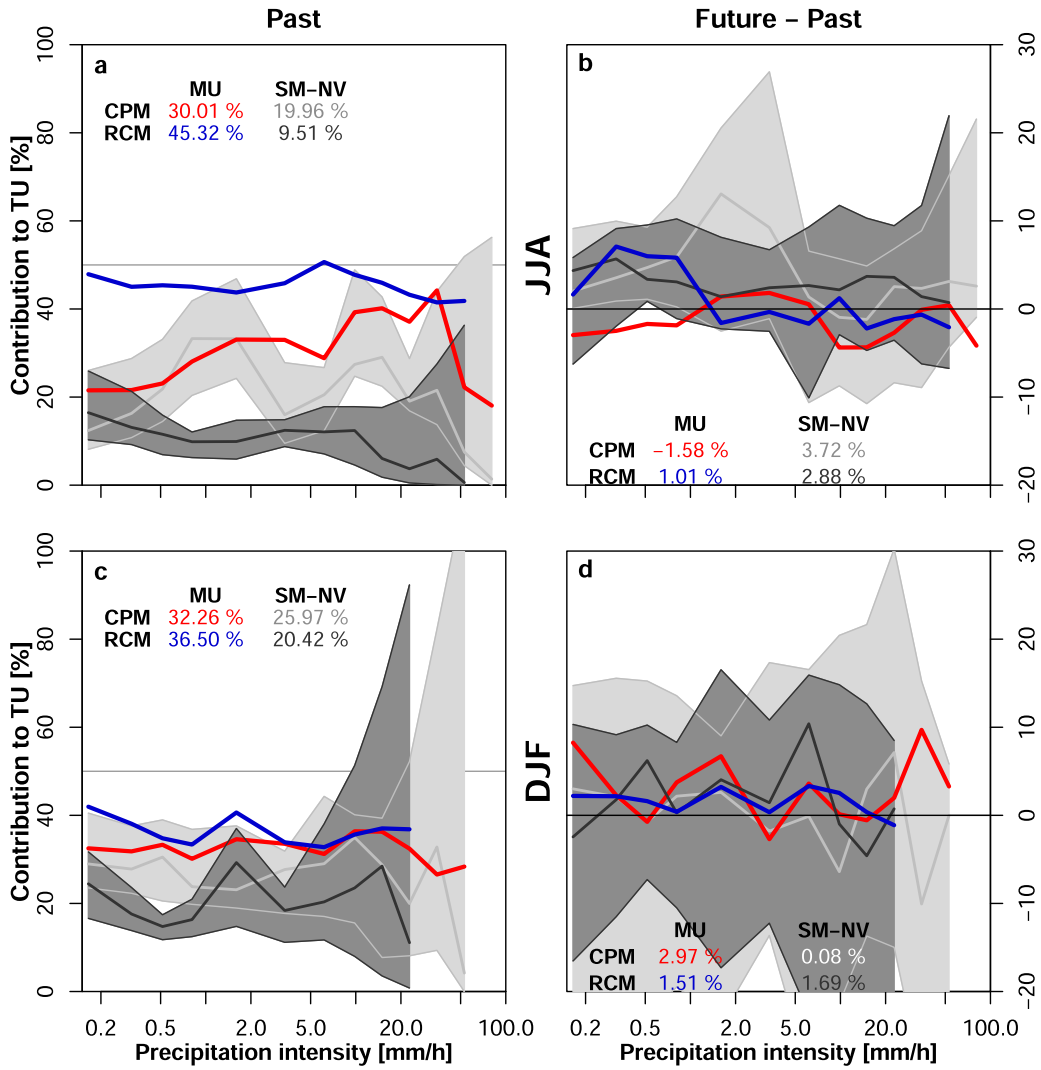

Fig. 4 | Model uncertainty contribution to total uncertainty in the fractional contribution of hourly precipitation intensities to the total precipitation. For the summer (panel **a**, **b**) and winter (panel **c**, **d**) in the past (panel **a**, **c**) and for future changes (panel **b**, **d**) model uncertainty (MU) contribution to total uncertainty (TU) for CPM (red) and RCM (blue) bootstrapped ensemble and the mean single-model natural variability (SM-NV) contribution to the TU for CPMs (light grey) and RCMs (dark grey) and its 95th confidence interval. In numbers the mean contribution to the TU for CPMs and RCMs both in the past and future changes. In all panels the statistics are calculated when at least 50% of the models have events in the bin.

For the past climate, both model and total uncertainty are substantially lower in the CPM than RCM ensemble except for extremes when the total uncertainty for the CPM becomes larger driven by the natural variability (Supplementary Fig. 2a). In the future the picture remains similar, but the RCMs show a stronger increase especially in model uncertainty for intensities above 5 mm/h compared to CPMs (Supplementary Fig. 2b). This could be linked to the intrinsic limitations of convection-parameterised models to correctly represent the intensification of convective events.

The contribution of the model uncertainty to the total uncertainty is substantially reduced in CPMs compared to RCMs with a mean contribution of 30% instead of 45.32% in the past and similarly in the future (Fig. 4a, b). This is even more evident for precipitation above 50 mm/h, where the CPM model uncertainty contribution drops to ~20% while for the RCM remains at ~50%. This reduction in the contribution from model uncertainty for the CPMs is likely to be linked to the explicit representation of convection. In fact, in DJF the model uncertainty can explain only between ~32% and ~36% of the total uncertainty for both CPMs and RCMs in either time slices and all precipitation intensities (Fig. 4c, d). It is notable that the contribution from model uncertainty is similar across both seasons for the CPMs, which is consistent with storms being resolved in both seasons; whilst for the RCM the contribution from model uncertainty is greater in summer when the convection parameterisation scheme (and its uncertainty) plays a significant role.

The natural variability sampled by a single model realisation (SM-NV) only explains a small portion of the total uncertainty of the multi-model ensemble both in the past and in the future. However, it is interesting that the SM-NV contribution to total uncertainty is on average more than double in CPMs compared to RCMs, and reaching more than 50% for extremes (Fig. 4). This confirms that natural variability is an important component of uncertainty especially in CPMs[4].

The findings are not linked to the specific models included in the ensemble. In fact, the above conclusions hold when considering subsamples of models from different families, although the model uncertainty contribution to the total uncertainty substantially increases (between 10 and 15%) for both CPMs and RCMs, while SM-NV contribution remains around the same range (Supplementary Figs. 3 and 4). In the future, while the contribution of model uncertainty for CPMs decreases for all the subsets (up to 3.4%), for RCMs increases or decreases depending on the set of chosen models showing the sensitivity of the RCMs to the model choice.

Up to now, we looked at future changes and related uncertainties from a climatological perspective (i.e., hourly intensity distribution). However, engineers and practitioners usually focus on precipitation events, characterising them by their intensity and duration, to identify and predict those leading to flooding. Here we define an event as a continuous period of precipitation exceeding 0.1 mm/hr and evaluate the future changes in the maximum precipitation intensity for different event durations (Fig. 3) and the related uncertainty (Fig. 5). Similar results are also found considering event total amounts rather than maximum intensity of the event (not shown). In line with previous findings[4,5], Fig. 3 shows an intensification of short-lived high-intensity events (i.e., duration below 6 h and intensities above 10 mm/h) along with a decrease of long-lasting low-intensity events. The model contribution to the total uncertainty in RCMs tends to be high (>40%) for precipitation above 10 mm/h and below 0.2 mm/h of short duration (Fig. 5). This highlights the intrinsic limitation of this resolution in representing short-lived high-intensity events[5] as well as very light precipitation, known as drizzle problem[6]. The contribution for this type of events is substantially reduced in CPMs, up to 20%, while on average across intensities and duration the reduction is of 6.7%. In the future, in contrast with RCMs, CPMs show a further reduction of model uncertainty contribution across all durations and intensities. The results hold also with different subsets of models, but the model contribution substantially increases especially for RCMs, which show a mean contribution above 50% for the subset CMCC, CNRM, ETH, FZJ-IDL, ICTP, MOHC versus the 35% in CPMs (Supplementary Figs. 5 and 6).

At this point it is interesting to identify if some areas within the domain are more prone to model uncertainties due to local processes, such as mechanically and thermally induced circulations associated with orography and coastal heterogeneities. The analysis is performed for heavy (p99) precipitation, defined at each grid point as the 99th quantile of wet hours based on the historical period. This threshold corresponds to the intensities that are projected to contribute the most to the total precipitation in the future (Fig. 2), but results hold also for extreme precipitation (p99.9, not shown). While the frequency of wet hours is expected to decrease in future summers (table in Supplementary Figure 1) especially over the Alps[15], the p99 intensity of wet hours shows a widespread increase over land in the future with a rise of almost 29% (24%) in CPM (RCM) ensemble corresponding to 2.75 mm/h (1.2 mm/h) on top of the current p99 value (Fig. 6). Care is needed to directly use this increase in impact-oriented assessment of changes since the analysis uses wet-hour percentiles[26].

In panel a and b, Fig. 7 shows that the model uncertainty, averaged over the grid points with significant future changes, is on average strongly reduced in CPMs compared to RCMs in the past as well as in the future (−16.28%, −5.73%). Compared to RCMs, higher model uncertainties are projected in the future for CPMs over the Alps. This could be linked to events that are more orographically induced[18] and thus less sensitive to the convective representation in future. In addition, the CPMs statistics could be affected by a "double-penalty problem"[6] due to their substantially higher spatial variability, more than double compared to RCMs (even when remapped on the RCM grid). In other words, CPMs agree on an increase in p99 over the Alps, but then diverge on the exact grid points where the increase occurs. The RCMs, that inherently have less variability across grid points, will suffer less from this problem. This suggests that a grid-point based assessment probably is not appropriate when dealing with CPMs and would instead support more a regional analysis and/or other statistical methods that account for such displacements.

We note that sea and coastal areas, where there is no significant climate change signal, show a higher model uncertainty in CPMs than in RCMs. This is probably linked with the rarity of the heavy precipitation especially over the Mediterranean sea, i.e. average frequency between 0.2 and 0.5 events per year in the historical period decreasing in the future. However, other factors could play a role like the inability of RCMs to advect inland maritime convective showers triggered over the sea[27], the different land-sea masks between CPMs and RCMs or a different treatment of sea-air interaction among CPMs. Despite these local regions showing higher model uncertainty in the CPMs, the model contribution to the total uncertainty is substantially reduced in CPMs almost uniformly over the domain by at least 22% (Fig. 7c, d), since the uncertainty is dominated by natural variability.

Discussion

In this work we investigated future changes in extreme hourly precipitation over the greater Alpine region in summer comparing the multi-model CPM ensemble, created within the FPS Convection project, with its driving convection-parametrised RCM ensemble. In accordance with previous literature, we find a good agreement in terms of future projections between the two ensembles, although the changes are larger in the CPMs. In particular, at the end of the century under the RCP8.5 scenario, the extreme precipitation events, especially of short duration, will become more intense and widespread over land with an increase of almost 29% compared to current values.

The main focus of this paper is however on the uncertainty linked with the climate change signal and, in particular, on the contribution of model uncertainty and natural variability to the total uncertainty within the RCP8.5 scenario. We found that, compared to RCMs, CPMs systematically reduce, in both the past and the future time slices, the contribution of model uncertainty to the total uncertainty that is dominated especially for the extremes by natural variability. This reduction appears to be linked to the explicit representation of convection, especially in summer; in fact in winter the model uncertainty contribution is similar between CPMs and RCMs in either time slices and all precipitation

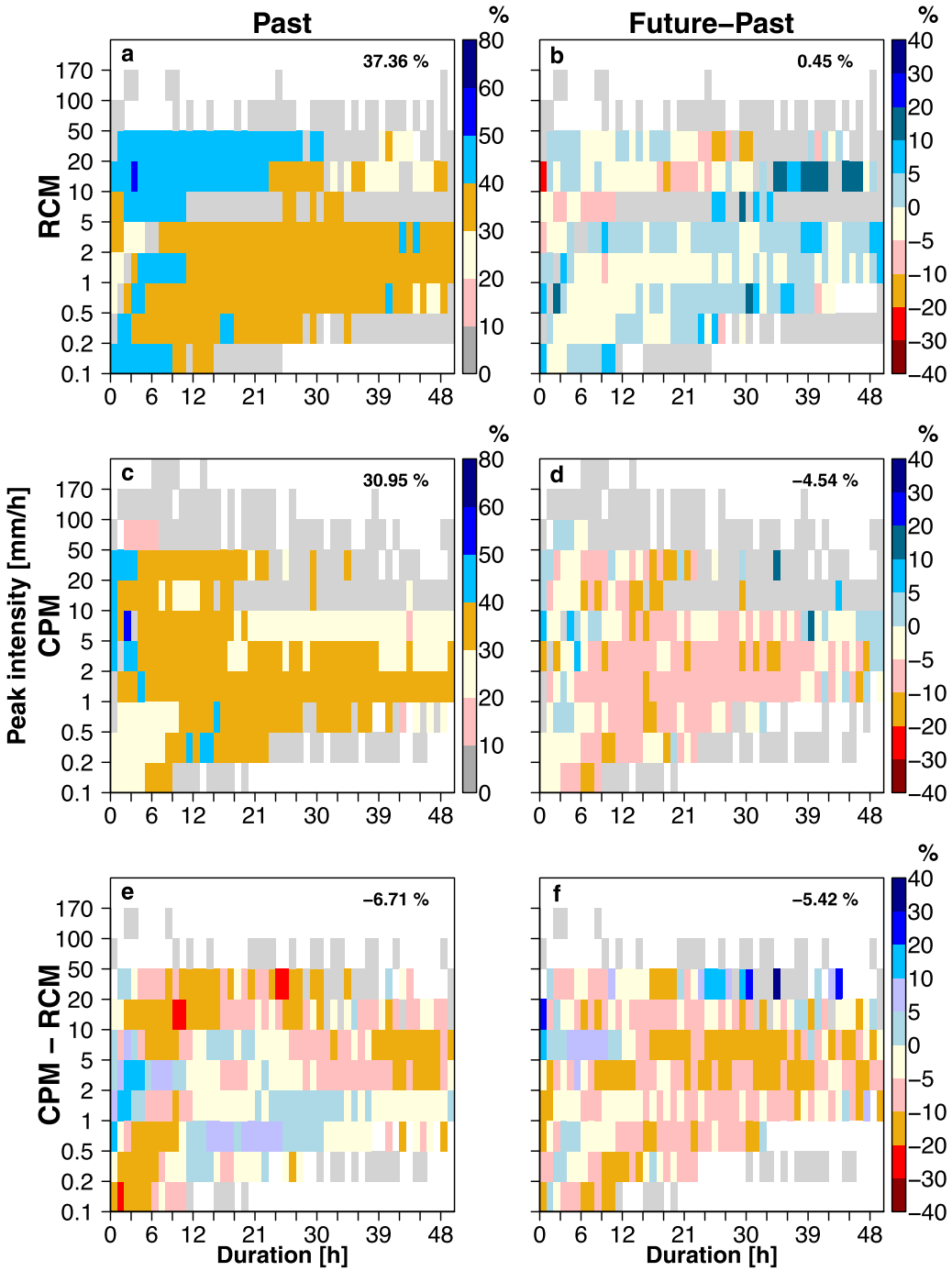

Fig. 5 | Model uncertainty contribution to total uncertainty in the precipitation event characteristics. Model contribution to total uncertainties for RCM (panel **a**, **b**), CPM (panel **c**, **d**) and CPM-RCM difference (panel **e**, **f**) bootstrapped ensemble for the past (panel **a**, **c**, **e**) and future changes (panel **b**, **d**, **f**) defined as future-past time slice. The model contribution to the total uncertainty is calculated for the fractional contribution of different events defined based on their peak precipitation intensity and duration in summer only when at least 50% of the models have events in that bin. An event is defined as a continuous period of precipitation exceeding 0.1 mm/h. The percentage in the plot represents the mean model contribution to the total uncertainty considering all duration and intensities with future changes significant at the 95th level.

intensities. This analysis also highlights the already well-known limitations of RCMs in representing short-lived high-intensity events as well as very light precipitation; in both cases the CPMs reduced the model uncertainty contribution up to 20%. This reduction in model uncertainty contribution is consistent over the domain, although model uncertainty can be higher in CPMs than in RCMs in some areas, like over the Alps, in the future. Importantly, the findings hold when considering subsamples of models from different families, thus proving that the results do not depend on selected models.

From our analysis, we conclude that CPMs not only project a stronger intensification of local extreme precipitation compared to RCMs but, even more importantly, the reduction of model uncertainty, for both the present climate and the future changes, is due to their more realistic representation of local dynamical processes. Knowing that the model uncertainty is reduced in the projections of both short-lived high-intensity and long-lasting events is key for flood modellers since the former tend to cause damaging urban flooding[28] and the latter can be of concern for large river basins, such as the Po valley in Italy[29]. Thus, reducing the contribution of

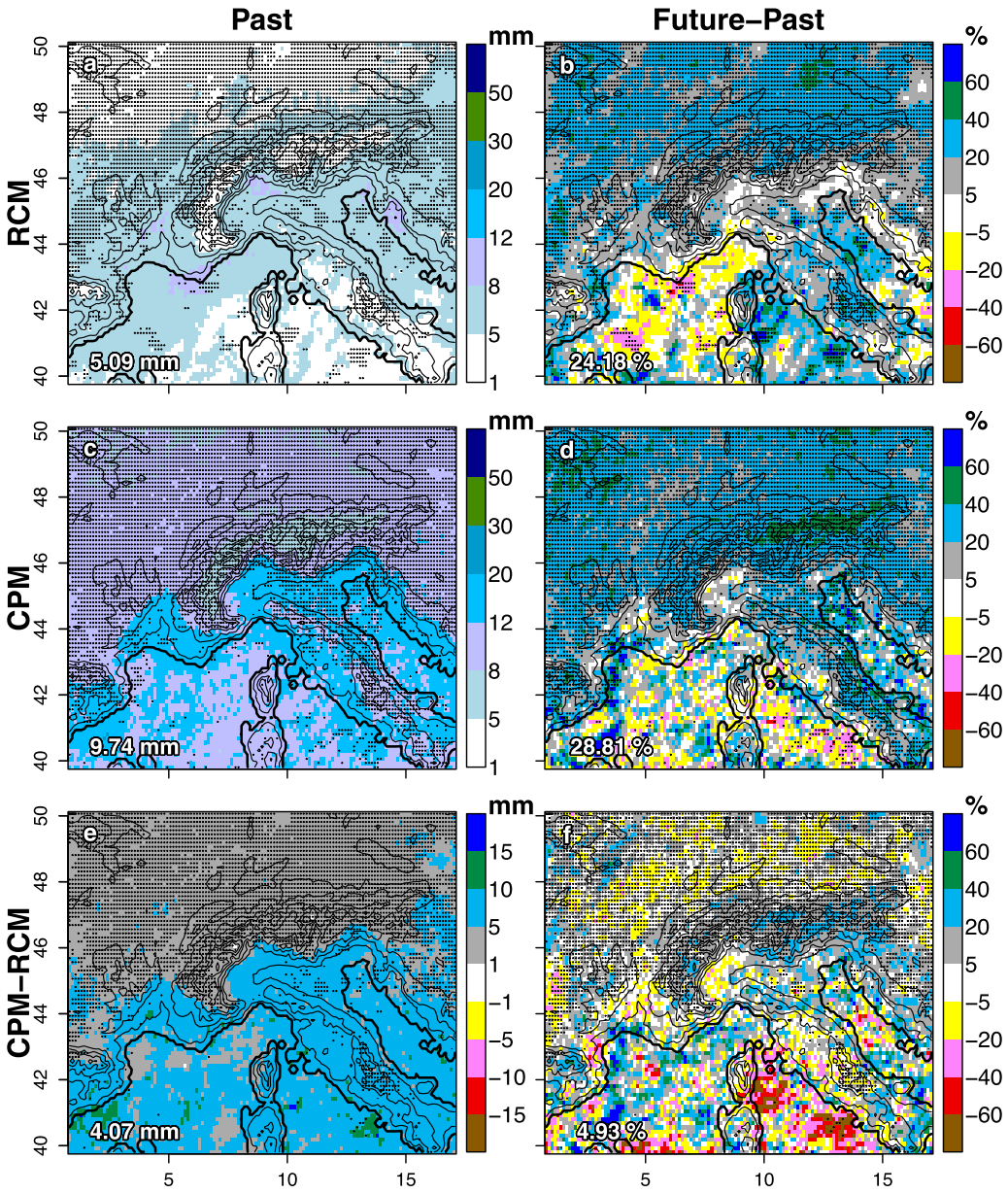

Fig. 6 | Maps of heavy precipitation for past and future changes. The heavy (p99) precipitation for RCM (panel **a**, **b**) and CPM (panel **c**, **d**) ensemble mean and CPM-RCM difference (panel **e**, **f**) for the past time slice (panel **a**, **c**, **e**) and future changes in percentage (panel **b**, **d**, **f**) is calculated considering only wet hours. Significant changes are identified by black dots for which the mean is calculated and shown in text.

model uncertainty to the total uncertainty is a crucial aspect for impact assessment models and policy makers that can now have the benefit of more certain extreme rainfall projections than ever before.

Methods

Data

Table 1 gives an overview of the nine models used and corresponding responsible institutes, who joined this analysis. All CPMs explicitly resolve deep convective processes, while for RCMs and GCMs the deep convection is parametrized. The RCMs span Europe with slightly different domain sizes, while CPMs have different domain size but all cover the common area for analysis (1E – 17E; 40 N – 50 N) defined in the FPS Convection protocol (see Fig. 1 in Coppola et al., 2020). To compare the outputs among each other and on equal terms[30], a conservative remapping to the a common 12 km grid is applied to all simulations before calculating the statistics. Each 10-year time slice is preceded by one (or two for CNRM-AROME41t1) spin-up year that is removed from the analysis. To note that the UKMO model uses different time slices, i.e., 1998–2007 and 2096–2105, and directly nested the CPM in a high-resolution GCM at 25 km resolution.

Bootstrapping strategy

The schematic of the bootstrapping strategy used to examine the uncertainties in the CPM and RCM ensembles is shown in Fig. 1. The nine models are represented by the vivid coloured cuboid, where the three dimensions are longitude, latitude and time with the original hourly resolution (Fig. 1 centre). To evaluate model uncertainties the 9 models are first randomly reassembled 9000 times with replacement; then the selected statistic, e.g. heavy precipitation p99, is applied to each of the 9000 bootstrap surrogates, thus reducing the cuboid to a square, called "calculated surrogate", with two dimensions, i.e. longitude and latitude (Fig. 1 left). The ensemble spread is calculated as difference between the 2.5th and 97.5th quantiles of the 9000 "calculated surrogates". To note that the model uncertainty includes the intrinsic natural variability of the original 10 years of data. Similarly, to

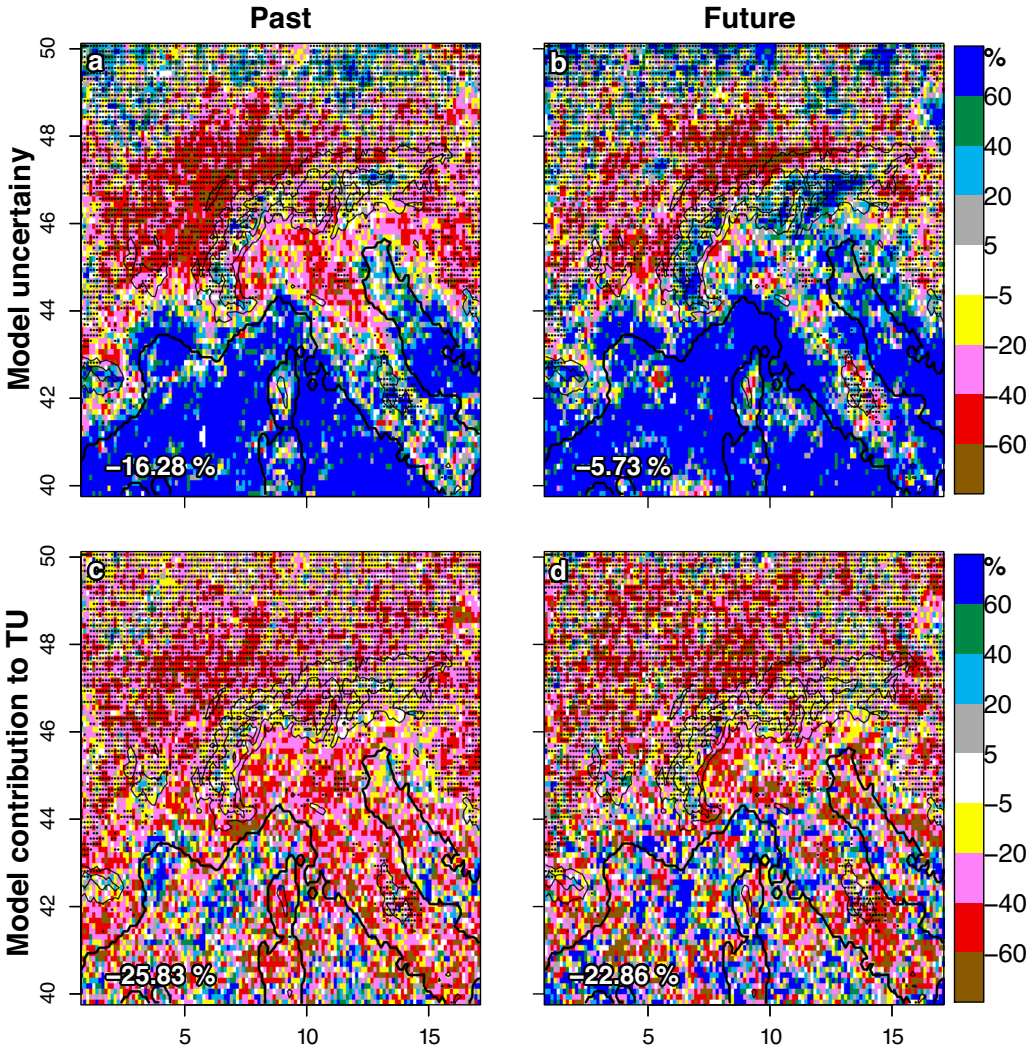

Fig. 7 | Maps of heavy precipitation model uncertainty and its contribution to total uncertainty. For heavy precipitation (p99) maps of: on panel **a** and **b**, percentage differences in model uncertainty between CPM and RCM bootstrapped ensemble, calculated as (CPM spread -RCM spread)/RCM spread*100; on panel **c** and **d**, the percentage differences in model contribution to total uncertainty between CPM and RCM bootstrapped ensemble. Negative (positive) values represent a decrease (increase) in model uncertainty and contribution to total uncertainty in CPMs compared to RCMs in the past (panel **a**, **c**) and future (panel **b**, **d**). In text for each plot the mean value over the grid points (black dots) with a significant future precipitation change at the 95th level.

investigate the natural variability of each model, called single-model natural variability (SM-NV), 1000 bootstrap surrogates are created by randomly selecting 10 years with replacement and the selected statistic is applied to each of the 1000 bootstrap surrogates (Fig. 1 right). To note that an initial-conditions larger ensemble of longer simulations would be required to evaluate the full range of internal variability[31], which might be limited in our case by the relatively short length of the simulations. For the calculation of the SM-NV, the years in the past and future time slices are ordered from 1 to 10 and, in each iteration of the bootstrapping, the same selection of 10 years is taken for both past and future time slices. Likewise for the bootstrapping of model uncertainty, the same selection of models is chosen for the past and the future for each surrogate. The spread in SM-NV is calculated for the same quantile interval as in the model uncertainty. The ensemble spread for the total uncertainties is calculated considering all "calculated surrogates" obtained for the SM-NV, thus over 9000 "calculated surrogates" (i.e., 9 members * 1000 bootstraps). With this strategy, total uncertainty includes the uncertainties related to both natural variability and model characteristics. To note that different methodologies for the calculation of the total uncertainty have been tested leading to the same results (see supplementary materials). Finally, the model contribution to the total uncertainty is calculated as the spread in model uncertainty divided by the spread in the total uncertainty multiplied by 100%. In the same way the SM-NV contribution to the total uncertainty is calculated for each model and displayed either as mean or/and as 95th confidence interval.

The bootstrap analysis is based on the hypothesis that the years and the models are equally plausible and independent realizations of the climate. While the assumption on the years is reasonable for short time scale (i.e. ten years), the model independency needs to be verified especially for CPMs from the same family and GCM forcing, i.e. COSMO (ETH and KIT) and AROME (CNRM, KNMI and DMI-MET-SMHI). For this purpose, the different statistics are repeated for a subset of models containing only one model for each family for both CPMs and RCMs.

Data availability

The hourly precipitation data of the CORDEX-FPS on Convection CP-RCMs ensemble are in the process of becoming available through the ESGF data notes.

Code availability

The codes to reproduce the analyses presented in this study are available upon request from the corresponding author.

Received: 22 September 2023; Accepted: 16 February 2024;
Published online: 28 February 2024

References

1. Giorgi, F. Thirty years of regional climate modeling: where are we and where are we going next? *J. Geophys. Res. Atmos.* **124**, 5696–5723 (2019).
2. Mearns, L. O., Lettenmaier, D. P. & McGinnis, S. Uses of results of regional climate model experiments for impacts and adaptation studies: the example of NARCCAP. *Curr. Clim. Chang. Rep.* **1**, 1–9 (2015).
3. Goergen, K. & Kollet, S. Boundary condition and oceanic impacts on the atmospheric water balance in limited area climate model ensembles. *Sci. Rep.* **11**, 6228 (2021).
4. Fosser, G., Kendon, E. J., Stephenson, D. & Tucker, S. Convection-permitting models offer promise of more certain extreme rainfall projections. *Geophys. Res. Lett.* **47**, 1–9 (2020).
5. Kendon, E. J. et al. Heavier summer downpours with climate change revealed by weather forecast resolution model (suppMat). *Nat. Clim. Chang.* **4**, 570–576 (2014).
6. Prein, A. F. et al. A review on regional convection-permitting climate modeling: demonstrations, prospects, and challenges. *Rev. Geophys.* **53**, 323–361 (2015).
7. Burt, S. Cloudburst upon Hendraburnick down: the Boscastle storm of 16 August 2004. *Weather* **60**, 219–227 (2005).
8. Fosser, G., Khodayar, S. & Berg, P. Benefit of convection permitting climate model simulations in the representation of convective precipitation. *Clim. Dyn.* **44**, 45–60 (2014).
9. Kendon, E. J. et al. Do convection-permitting regional climate models improve projections of future precipitation change? *Bull. Am. Meteorol. Soc.* **98**, 79–93 (2017).
10. Hawkins, E. & Sutton, R. The potential to narrow uncertainty in regional climate predictions. *Bull. Am. Meteorol. Soc.* **90**, 1095–1107 (2009).
11. Tebaldi, C. & Knutti, R. The use of the multi-model ensemble in probabilistic climate projections. *Philos. Trans. R. Soc. A Math. Phys. Eng. Sci.* **365**, 2053–2075 (2007).
12. Déqué, M. et al. The spread amongst ENSEMBLES regional scenarios: Regional climate models, driving general circulation models and interannual variability. *Clim. Dyn.* **38**, 951–964 (2012).
13. Kendon, E. J. et al. UKCP Convection-permitting model projections: Science report. 1–153 https://www.metoffice.gov.uk/pub/data/weather/uk/ukcp18/science-reports/UKCP-Convection-permitting-model-projections-report.pdf (2019).
14. Coppola, E. et al. A first-of-its-kind multi-model convection permitting ensemble for investigating convective phenomena over Europe and the Mediterranean. *Clim. Dyn.* **55**, 3–34 (2020).
15. Pichelli, E. et al. The first multi-model ensemble of regional climate simulations at kilometer-scale resolution part 2: historical and future simulations of precipitation. *Clim. Dyn.* **56**, 3581–3602 (2021).
16. Ban, N. et al. The first multi-model ensemble of regional climate simulations at kilometer-scale resolution, part I: evaluation of precipitation. *Clim. Dyn.* **57**, 275–302 (2021).
17. Ha, M. T. et al. Precipitation frequency in Med-CORDEX and EURO-CORDEX ensembles from 0.44° to convection-permitting resolution: impact of model resolution and convection representation. *Clim. Dyn*. https://doi.org/10.1007/s00382-022-06594-6 (2022).
18. Müller, S. K. et al. The climate change response of alpine-mediterranean heavy precipitation events. *Clim. Dyn.* **62**, 165–186 (2024).
19. Soares, P. M. M. et al. The added value of km-scale simulations to describe temperature over complex orography: the CORDEX FPS-Convection multi-model ensemble runs over the Alps. *Clim. Dyn*. https://doi.org/10.1007/s00382-022-06593-7 (2022).
20. Müller, S. K. et al. Evaluation of Alpine-Mediterranean precipitation events in convection-permitting regional climate models using a set of tracking algorithms. *Clim. Dyn.* **61**, 939–957 (2023).
21. Riahi, K. et al. RCP 8.5—A scenario of comparatively high greenhouse gas emissions. *Clim. Change* **109**, 33–57 (2011).
22. Efron, B. & Tibshirani, R. J. An Introduction to the Bootstrap. in *CRC Monographs on Statistics and Applied Probability* (ed. Chapman & Hall (Eds.)) (Chapman & Hall, 1993).
23. Klingaman, N. P., Martin, G. M. & Moise, A. ASoP (v1.0): a set of methods for analyzing scales of precipitation in general circulation models. *Geosci. Model Dev.* **10**, 57–83 (2017).
24. Berthou, S. et al. Pan-European climate at convection-permitting scale: a model intercomparison study. *Clim. Dyn.* **55**, 35–59 (2020).
25. Prein, A. F. et al. The future intensification of hourly precipitation extremes. *Nat. Clim. Chang.* **7**, 48–52 (2017).
26. Schär, C. et al. Percentile indices for assessing changes in heavy precipitation events. *Clim. Change* **137**, 201–216 (2016).
27. Kendon, E. J. et al. Greater Future U.K. Winter Precipitation Increase in New Convection-Permitting Scenarios. *J. Clim.* **33**, 7303–7318 (2020).
28. Zhou, Z. et al. The complexities of urban flood response: Flood frequency analyses for the Charlotte metropolitan region. *Water Resour. Res.* **53**, 7401–7425 (2017).
29. Montanari, A. Hydrology of the Po River: looking for changing patterns in river discharge. *Hydrol. Earth Syst. Sci.* **16**, 3739–3747 (2012).
30. Berg, P., Wagner, S., Kunstmann, H. & Schädler, G. High resolution regional climate model simulations for Germany: part I—validation. *Clim. Dyn.* **40**, 401–414 (2013).
31. Deser, C. et al. Insights from Earth system model initial-condition large ensembles and future prospects. *Nat. Clim. Chang.* **10**, 277–286 (2020).
32. Rockel, B., Will, A. & Hense, A. The Regional Climate Model COSMO-CLM (CCLM). *Meteorol. Z.* **17**, 347–348 (2008).
33. Adinolfi, M., Raffa, M., Reder, A. & Mercogliano, P. Evaluation and Expected Changes of Summer Precipitation at Convection Permitting Scale with COSMO-CLM over Alpine Space. *Atmosphere (Basel).* **12**, 54 (2020).
34. Sørland, S. L. et al. COSMO-CLM regional climate simulations in the Coordinated Regional Climate Downscaling Experiment (CORDEX) framework: a review. *Geosci. Model Dev.* **14**, 5125–5154 (2021).
35. Baldauf, M. et al. Operational convective-scale numerical weather prediction with the COSMO model: Description and sensitivities. *Mon. Weather Rev.* **139**, 3887–3905 (2011).
36. Keuler, K., Radtke, K., Kotlarski, S. & Lüthi, D. Regional climate change over Europe in COSMO-CLM: Influence of emission scenario and driving global model. *Meteorol. Z.* **25**, 121–136 (2016).
37. Leutwyler, D., Fuhrer, O., Lapillonne, X., Lüthi, D. & Schär, C. Towards European-scale convection-resolving climate simulations with GPUs: a study with COSMO 4.19. *Geosci. Model Dev.* **9**, 3393–3412 (2016).
38. Leutwyler, D., Lüthi, D., Ban, N., Fuhrer, O. & Schär, C. Evaluation of the convection-resolving climate modeling approach on continental scales. *J. Geophys. Res. Atmos.* **122**, 5237–5258 (2017).
39. Caillaud, C. et al. Modelling Mediterranean heavy precipitation events at climate scale: an object-oriented evaluation of the CNRM-AROME convection-permitting regional climate model. *Clim. Dyn.* **56**, 1717–1752 (2021).
40. Nabat, P. et al. Modulation of radiative aerosols effects by atmospheric circulation over the Euro-Mediterranean region. *Atmos. Chem. Phys.* **20**, 8315–8349 (2020).
41. Belušić, D. et al. HCLIM38: a flexible regional climate model applicable for different climate zones from coarse to convection-permitting scales. *Geosci. Model Dev.* **13**, 1311–1333 (2020).
42. Noël, B. et al. Evaluation of the updated regional climate model RACMO2.3: summer snowfall impact on the Greenland Ice Sheet. *Cryosphere* **9**, 1831–1844 (2015).

43. Powers, J. G. et al. The Weather Research and Forecasting Model: Overview, System Efforts, and Future Directions. *Bull. Am. Meteorol. Soc.* **98**, 1717–1737 (2017).
44. Coppola, E. et al. Non-Hydrostatic RegCM4 (RegCM4-NH): model description and case studies over multiple domains. *Geosci. Model Dev.* **14**, 7705–7723 (2021).
45. Chan, S. C. et al. Europe-wide precipitation projections at convection-permitting scale with the Unified Model. *Clim. Dyn.* **55**, 409–428 (2020).

Acknowledgements

We acknowledge the WCRP-CORDEX-FPS on Convective phenomena at high resolution over Europe and the Mediterranean (FPSCONV-ALP-3). The work presented in this paper has been developed within the framework of the project "Dipartimento di Eccellenza 2023–2027", funded by the Italian Ministry of Education, University and Research at IUSS Pavia. This work was supported by CARIPARO Foundation through the Excellence Grant 2021 to the "Resilience" Project. We thank the research data exchange infrastructure and services provided by the Jülich Supercomputing Centre, Germany, as part of the Helmholtz Data Federation initiative. For the contribution from Research Centre Jülich, the authors gratefully acknowledge computing time on the supercomputer JURECA at Forschungszentrum Jülich. EJK gratefully acknowledges funding from the Joint U.K. BEIS/Defra Met Office Hadley Centre Climate Programme (GA01101). NB and MED acknowledge the Partnership for Advanced Computing in Europe (PRACE) for awarding them access to Piz Daint at the Swiss National Supercomputing Centre (CSCS, Switzerland); they also acknowledge the Federal Office for Meteorology and Climatology (MeteoSwiss), CSCS, the Center for Climate Systems Modeling (C2SM), and ETH Zürich for their contributions to the development and maintenance of the GPU-accelerated version of COSMO. The RegCM simulations for the ICTP institute have been completed thanks to the support of the CINECA supercomputing center, Bologna, Italy. Part of the simulations used in this study have been produced in the EUCP project, EUCP is financed by the European Commission through the Horizon 2020 Programme for Research & Innovation, Grand Agreement, 776613.

Author contributions

G.F. conceived the idea and performed the analysis on the CPMs and RCMs climate data provided by E.J.K., M.A., N.B., D.B., C.C., J.A.M.C, E.C., M.-E.D., H.dV., A.D., H.F., K.G., G.L., E.P., C.S., P.M.M.S., S.S. and M.H.T. G.F. wrote the manuscript with inputs from all co-authors.

Competing interests

The authors declare no competing interests.

Additional information

Supplementary information The online version contains supplementary material available at https://doi.org/10.1038/s41612-024-00600-w.

Correspondence and requests for materials should be addressed to Giorgia Fosser.